Environmental Science & Technology

Article

pubs.acs.org/est

Isotopically Modified Nanoparticles for Enhanced Detection in Bioaccumulation Studies

Superb K. Misra,[†,*] Agnieszka Dybowska,[†] Deborah Berhanu,[†] Marie Noële Croteau,[‡] Samuel N. Luoma,[‡] Aldo R. Boccaccini,[§] and Eugenia Valsami-Jones[∥,†]

[†]Natural History Museum, Dept. of Mineralogy, Cromwell Road, London SW7 5BD, United Kingdom

[‡]U.S. Geological Survey, Menlo Park, California, United States of America

[§]University of Erlangen-Nuremberg, Dept. of Materials Science, Erlangen 91058, Germany

[∥]School of Geography, Earth & Environmental Sciences, University of Birmingham, Edgbaston, B15 2TT, United Kingdom

Supporting Information

ABSTRACT: This work presents results on synthesis of isotopically enriched (99% ^{65}Cu) copper oxide nanoparticles and its application in ecotoxicological studies. ^{65}CuO nanoparticles were synthesized as spheres (7 nm) and rods (7 × 40 nm). Significant differences were observed between the reactivity and dissolution of spherical and rod shaped nanoparticles. The extreme sensitivity of the stable isotope tracing technique developed in this study allowed determining Cu uptake at exposure concentrations equivalent to background Cu concentrations in freshwater systems (0.2−30 μg/L). Without a tracer, detection of newly accumulated Cu was impossible, even at exposure concentrations surpassing some of the most contaminated water systems (>1 mg/L).

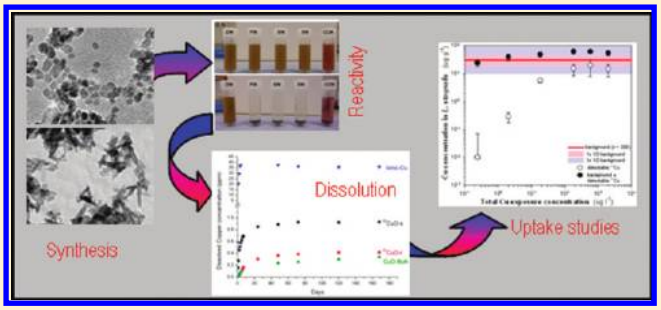

INTRODUCTION

Evaluating biological response to nanoparticles (NPs) at environmentally realistic concentration has become a pivotal point in the field of nanosafety. Understanding how particle characteristics affect bioaccumulation processes is an influential step in ascertaining biological impacts.[1] Various regulatory bodies and a US Environmental white paper on nanotechnologies in 2007 recommended careful tracking of uptake and accumulation of NPs to understand, for example, toxicity as a function of dose at the site of action.[2] Working with well-characterized particles is important in evaluating how physicochemical particle characteristics affect bioaccumulation. But an important challenge encountered with metal containing (e.g., metallic, metal oxides, metal sulphides) NPs is to differentiate between the background metal concentration and the newly accumulated metal resulting from exposure to NPs.[3] This problem is especially acute in the case of elements essential to organisms such as copper or zinc, which naturally occur in relatively high concentrations in biological tissues. One solution to tracking metal uptake is to label the metal with (i) radio isotopes, (ii) label the NP with dyes/phase contrasting agents, or (iii) label with an enriched stable isotope. Use of a label is especially critical if the goal is to work at the relatively low concentrations, which would be expected to characterize contaminated environments.[4] Issues exist with the reliable attachment of certain labels on NPs, with quantifying uptake with some types of labels and with the handling of radioactive materials. The use of an enriched stable isotope, if successful, provides a powerful and reliable alternative for detection and quantification of engineered NPs following short time exposures even at environmentally realistic concentrations.[4−6] Methods for the synthesis of particles with a stable isotope label remains understudied however.

Copper oxide nanoparticles (CuO NPs) are of interest due to their increasing use in various applications (such as catalysts, microelectronics, gas sensors, heat transfer fluids, high temperature superconductivity, batteries, and solar energy). There are also recent reports of possible bactericidal properties of CuO NPs,[7] which could result in CuO NPs being incorporated as fillers in various substrate/matrices.[8] Several studies have shown CuO NPs to induce significantly higher toxicity compared to bulk CuO particles to yeast,[9] algae,[10] and mammalian cell lines.[11,12] This is likely due to a combination of dissolved species generated from the NPs[13] and ROS (reactive oxygen species) mediated oxidative stress[14] thought to be an outcome of direct exposure to CuO NPs. In order to gain a mechanistic understanding of nano-CuO toxicity and assess the levels of bioaccumulation with certainty, it is imperative to determine the uptake and toxicity of CuO NPs at environmentally/physiologically realistic concentration. However, the background levels of Cu that occur in most biological tissues impede such studies.

Received: November 8, 2011
Revised: December 6, 2011
Accepted: December 7, 2011
Published: December 7, 2011

   dx.doi.org/10.1021/es2039757 | Environ. Sci. Technol. 2012, 46, 1216−1222

In the present work, a series of experiments were conducted to establish a simple protocol for synthesis of isotopically enriched copper oxide NPs (^{65}CuO). We show that the protocol can be used to produce particles with different physicochemical properties (e.g., shapes, dissolution), and we demonstrate how the stable isotope label enhances detection of net Cu accumulation in a model aquatic organism after exposure to a wide range of concentrations of isotopically modified ^{65}CuO NPs.

EXPERIMENTAL SECTION

Synthesis of ^{65}CuO NPs. Isotopically enriched $^{65}CuCl_2.2H_2O$ with 99% enrichment was purchased form Trace Sciences, USA. Isotopically modified (^{65}CuO) NPs with two different shapes (spheres and rods) were synthesized using wet chemistry. For ^{65}CuO-s NPs, 0.02 M of $CuCl_2.2H_2O$ was dissolved in 150 mL water and 500 μL of glacial acetic acid was added to the solution. The solution was then heated to 100 °C followed by a rapid addition of 0.6 g NaOH. This resulted in formation of a black precipitate, which was centrifuged out and repeatedly washed with water to get phase pure copper oxide NPs. ^{65}CuO-r NPs were obtained following a similar procedure in the absence of acetic acid. Micron sized CuO particles was purchased from Sigma Aldrich (U.K.).

Characterization Studies. Synthesized NPs were washed three times in deionized water prior to further characterization. Diluted suspension of the NPs was deposited on copper grid for TEM imaging (Hitachi 7100, 100 kV). The hydrodynamic size and zeta potential of the NPs were measured using Malvern Zetasizer (Malvern Instruments) at a concentration of 750 mg/L in water and at 22 °C. X-ray diffraction was performed on the NPs using Enraf-Nonius diffractometer coupled to INEL CPS 120 position-sensitive detector with Co−K_α radiation and the phase identification was performed using STOE software. For AFM measurements, diluted ^{65}CuO suspensions was deposited onto glass slide and allowed to air-dry in a clean environment. Atomic force microscopy (AFM) was conducted on the samples, using Asylum MFP-3D-SA (Santa Barbara, USA) instrument in AC mode. The samples were scanned in air using an Olympus AC-240TS tip (spring constant 2 N/m). ICP-AES (Varian Instruments) analysis was performed to determine the initial concentration of the copper oxide NPs aqueous suspension and also measure the dissolution of the NPs.

Reactivity and Copper Release Studies. All reactivity studies were conducted using copper concentration of 750 mg/L. The effect of temperature on zeta potential and hydrodynamic size of ^{65}CuO NPs was measured in deionized water using Malvern Zetasizer (Malvern Instruments). The effect of pH (Point of Zero charge) on the colloidal stability was measured in water for ^{65}CuO-r and ^{65}CuO-s NPs. The effect of adding ^{65}CuO NPs suspension in different environmental (fresh water, estuarine water, seawater) and biological media (cell culture media) was also investigated. Dissolution study was performed on the NPs by placing 10 mL of ^{65}CuO NPs suspension (in water) inside a dialysis bag (MWCO = 12.4 kDa) and transferring it to 250 mL plastic bottles (Nalgene) containing 200 mL of 1 mM $NaNO_3$ (pH = 6.7). The starting ^{65}CuO concentration inside the dialysis bag for the dissolution experiment was kept at 750 mg/L. Appropriate blanks were also included in the experimental set up to control for a potential contamination from reagents and containers. Soluble copper nitrate was used as the source of ionic copper. The bottles were incubated in 25 °C and at 200 rpm. Aliquots of 1 mL were taken from the media outside the dialysis bag at regular interval, acidified with 5% HNO_3 and the concentration of copper was then measured using ICP-AES. At the end of the dissolution experiment, suspensions inside the dialysis bag were examined under TEM to ascertain the presence of particles.

Biological Studies. Acute waterborne exposures[4] were conducted using the isotopically modified ^{65}CuO NPs in moderately hard water (US EPA 2002). Snails (*Lymnaea stagnalis*) of a restricted size range (mean dry weight of 13.4 ± 1.9 mg 95% CI, n = 47) were exposed for 24 h to a range of Cu concentrations in acid-washed 1 L HDPE containers. After exposure snails were sacrificed, digested and analyzed as described by Croteau et al.[4] Before and after exposure, water samples were taken from each vial, acidified (Baker Ultrex II grade, 2% HNO_3 final concentrations) and analyzed by ICP-MS. We used an isotope tracing technique that allows tracking newly accumulated tracers, independently from background levels.[4] Briefly, the relative abundance of ^{65}Cu tracer (i.e., p^{65}) is determined using the signal intensities of each isotope in the calibration standards, i.e.,

$$p^{65} = \text{Intensity}\left(\frac{^{65}\text{Cu}}{^{65}\text{Cu} + {}^{63}\text{Cu}}\right) \quad (1)$$

Concentrations of tracer in the exerimental organisms ($[^{65}Cu]_{\hat{e}}$) are calculated as the product of p^{65} and the total metal concentrations inferred by the ICP-MS software from tracer intensity ($[T^{65}Cu]$), i.e.,

$$[^{65}Cu]_{\hat{e}} = p^{65} x [T^{65}Cu] \quad (2)$$

The original load of tracer ($[^{65}Cu]_{\hat{e}}^{0}$) that occurred in each sample in the absence of a spike is calculated as the product of p^{65} and the total metal concentrations inferred from the intensity of the most abundant isotope ($[T^{63}Cu]$), i.e.,

$$[^{65}Cu]_{\hat{e}}^{0} = p^{65} x [T^{63}Cu] \quad (3)$$

The net tracer uptake ($\Delta[^{65}Cu]_{\hat{e}}$) is derived from the total experimental metal concentration ($[^{65}Cu]_{\hat{e}}$, eq 2) minus the pre-existing concentration of tracer ($[^{65}Cu]_{\hat{e}}^{0}$, eq 3).

RESULTS AND DISCUSSION

Characterization of ^{65}CuO NPs. Copper chloride was chosen as the precursor for synthesis of the NPs. Copper chloride can be obtained in isotopically enriched form (^{65}Cu) and is an appropriate chemical species for synthesizing ^{65}CuO NPs or nonisotopically modified CuO NPs. This precursor also offers the possibility of manipulating the synthesis technique to allow controlling the shape of the synthesized NPs (Figure 1). TEM images (Figure 1a) show that the spherical NPs had a size of 7 ± 1 nm and appear to be uniform in size and in a nonaggregated state. The spherical nature of ^{65}CuO-s NPs was also confirmed through atomic force microscopy (AFM) imaging (Figure 1c,d), which shows the height of the particles to be 9 ± 1 nm. In the case of nanorods, (Figure 1b) TEM size of the particles was found to be of 7 ± 1 nm in their width and 40 ± 10 nm in their length. Compared with the spheres, there was more size polydispersity in the length of the rods and they were highly agglomerated. The height of individual nanorods determined by AFM was 8 ± 1 nm (Figure 1d). The hydrodynamic size of ^{65}CuO-s NPs measured using dynamic light

dx.doi.org/10.1021/es2039757 | Environ. Sci. Technol. 2012, 46, 1216−1222

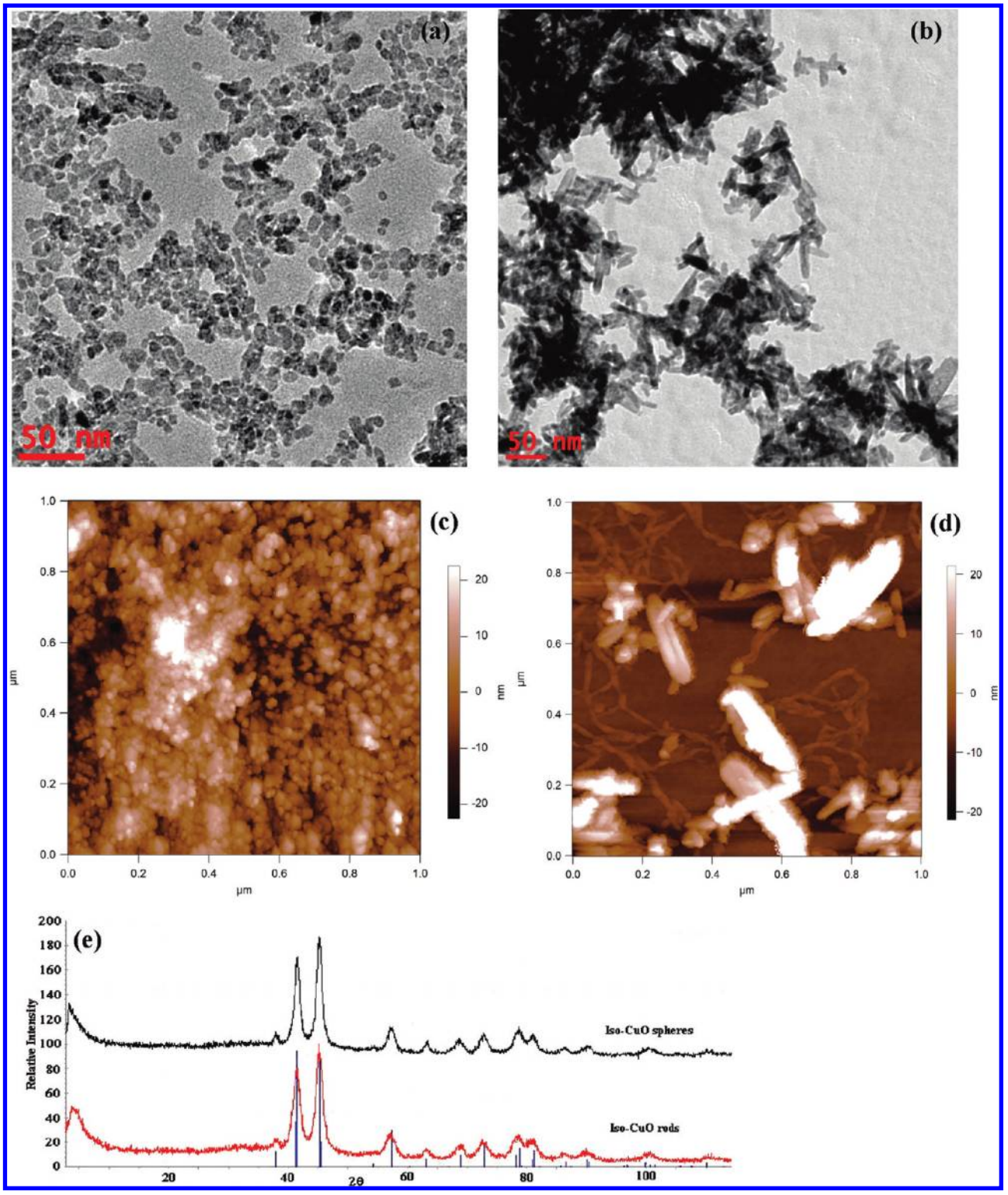

Figure 1. TEM images of (a) ^{65}CuO-s NPs, (b) ^{65}CuO-r NP. Atomic force microscopy (AFM) images of (c) ^{65}CuO-s NPs and (d) ^{65}CuO-r NPs. (e) X-ray diffraction pattern of the synthesized ^{65}CuO-s and ^{65}CuO-r NPs. The crystal phase identified for the particles was of Tenorite (ICDD 48-1548).

scattering (DLS) was found to be 82 ± 1 nm. No DLS measurement of ^{65}CuO-r NPs was performed due to the nature of the NPs (rods) and also its high tendency to agglomerate. The crystal phase identified by XRD for all the NPs was of Tenorite (ICDD 48- 1548) (Figure 1e). The specific surface area for the ^{65}CuO-s and ^{65}CuO-r NPs were 60 and 51 m^2/g, respectively. The synthesis method used in this study to prepare ^{65}CuO NPs was also employed to prepare nonisotopically modified CuO NPs, and the characterization results showed very similar size, shape and other physicochemical properties (data not shown).

Reactivity Studies. The stability of the NP suspension in various media was assessed using zeta potential measurements. Both ^{65}CuO-s and ^{65}CuO-r NPs indicated high stability in

dx.doi.org/10.1021/es2039757 | Environ. Sci. Technol. 2012, 46, 1216–1222

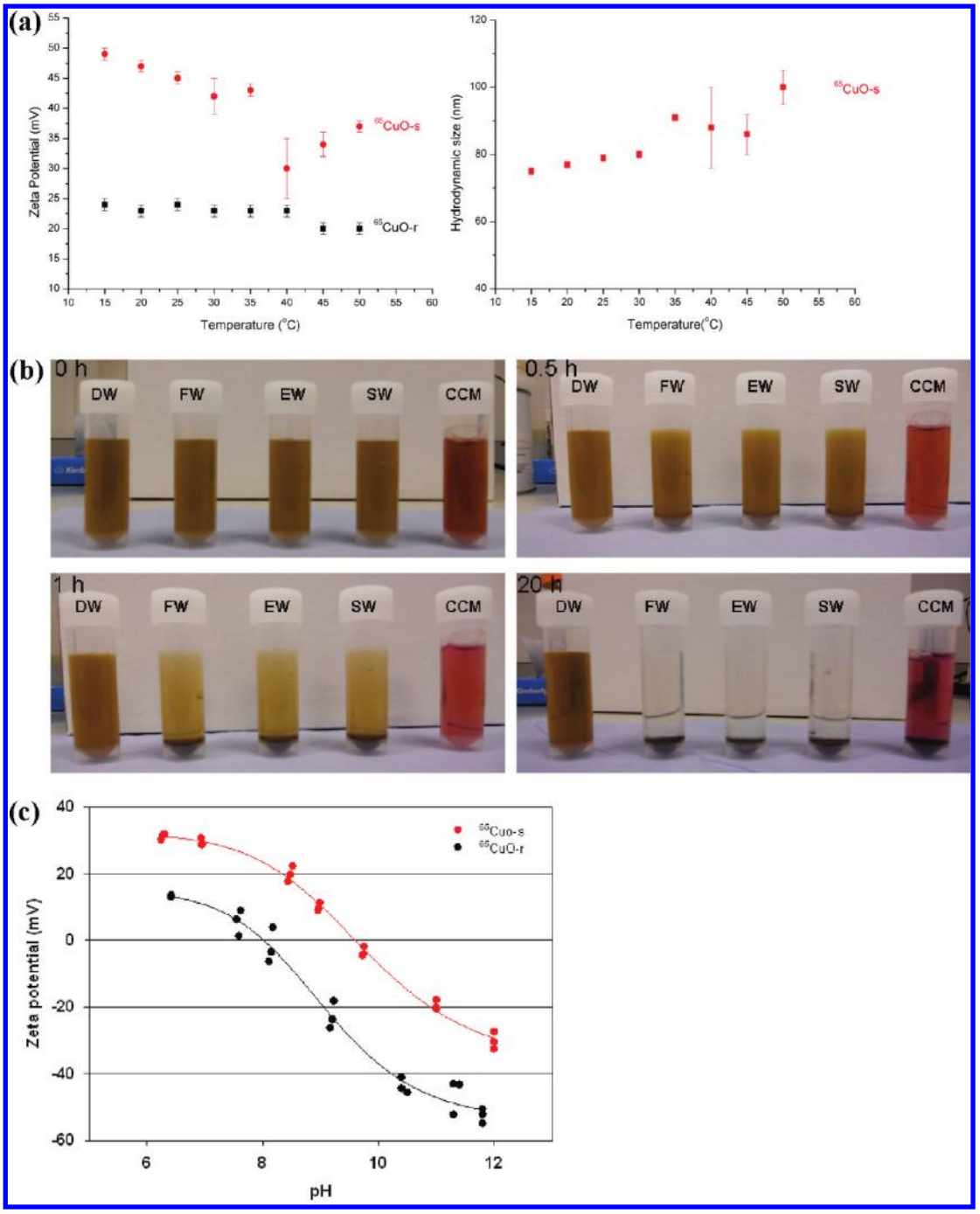

Figure 2. Effect of temperature on (a) zeta potential for ^{65}CuO-s and ^{65}CuO-r NPs and hydrodynamic size of ^{65}CuO-s NPs in water. (b) Digital images of ^{65}CuO-s NPs in various media (deionized water (DW), fresh water (FW), estuarine water (EW), seawater (SW), and cell culture media (CCM)) at different time points, showing the agglomeration of ^{65}CuO-s NPs. (c) Point of zero charge measurements for the ^{65}CuO-s and ^{65}CuO-r NPs in 1 mM $NaNO_3$ media at 22 °C.

deionized water with a positively charged zeta potential value of 42 ± 1 mV and 24 ± 1 mV, respectively. The relatively lower zeta potential of ^{65}CuO-r NPs compared to ^{65}CuO-s NPs indicates the higher potential for nanorod samples to agglomerate, explaining the suspension instability. Increasing the temperature caused an increase in the hydrodynamic size for ^{65}CuO-s NPs (Figure 2a) and a decrease in the zeta potential. However, there was no significant effect of temperature (within 15−50 °C) on the tendency to agglomerate for ^{65}CuO-r NPs. In contrast, an opposite effect of the media on the stability of NPs suspension was observed. As shown in Figure 2b, ^{65}CuO-s NPs suspension was stable in deionized water for up to 20 h, whereas in simulated environmental media (fresh water (FW), estuarine water (EW), seawater (SW)) and cell culture media (CCM) the particles agglomerated and started to sediment in the suspension within an hour. This observation was also reflected in the zeta potential measurements of CuO-s NPs, wherein very low zeta potential values were recorded in the environmental (+5 mV in FW, +4 mV in EW, and +2 mV in SW) and cell culture media (−10 mV). Additionally, the effect of pH on the stability of ^{65}CuO-s and ^{65}CuO-r NPs suspension in 1 mM $NaNO_3$ at 22 °C was also measured and is shown in

dx.doi.org/10.1021/es2039757 | Environ. Sci. Technol. 2012, 46, 1216−1222

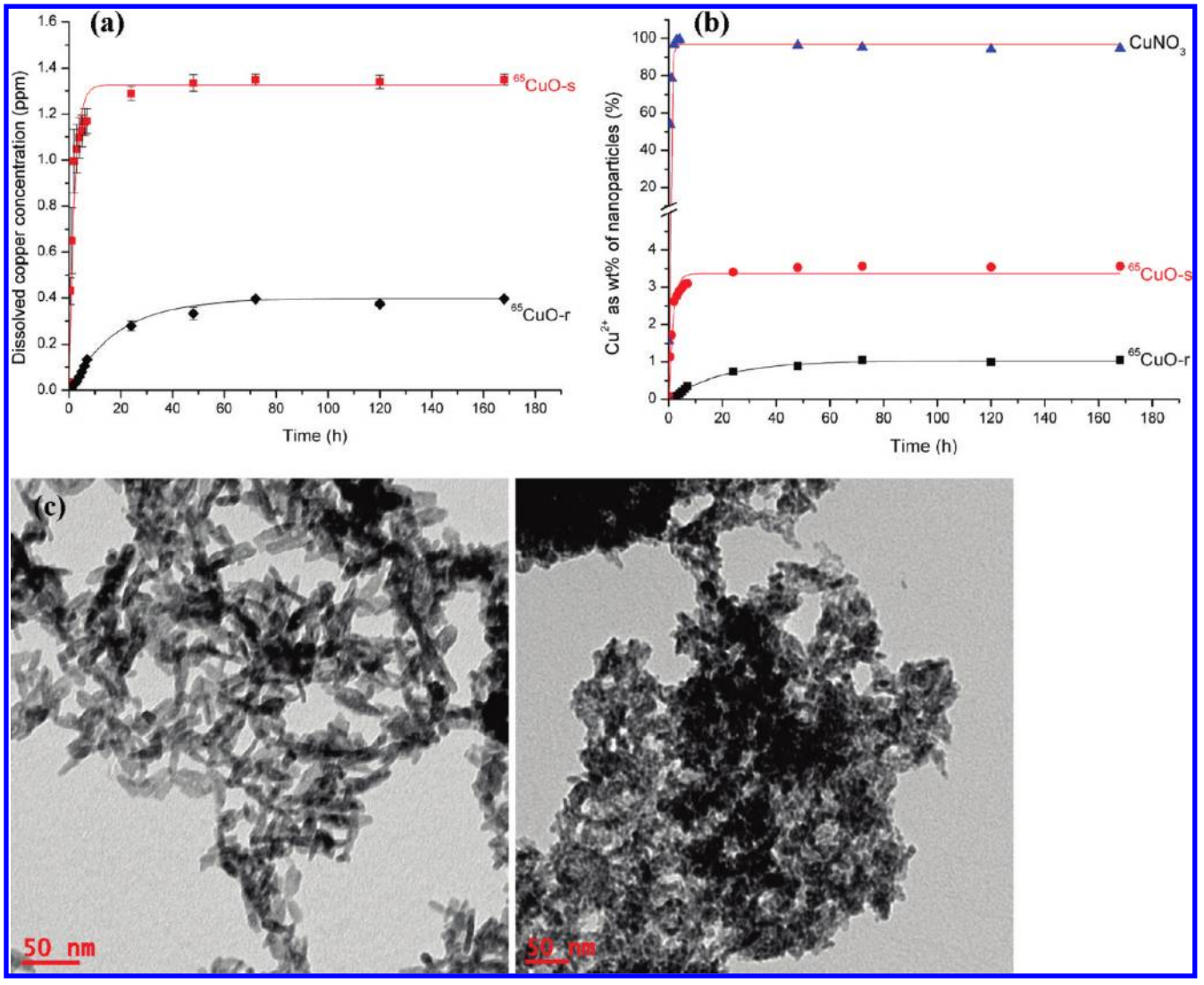

Figure 3. Dissolved Cu^{2+} release from copper oxide NPs in 1 mM $NaNO_3$ at 25 °C (a) expressed in concentration for ^{65}CuO-s and ^{65}CuO-r NPs, (b) expressed in proportion to the original concentration of NPs (mass %) for ^{65}CuO-s, ^{65}CuO-r NPs and recovery of copper from ionic copper used as a control for the dissolution study. The starting Cu concentration inside the dialysis bag for all the dissolution experiments were kept constant at 750 mg/L and all data were fitted with a first order exponential growth equation. TEM images of (c) ^{65}CuO-r and ^{65}CuO-s NPs from inside the dialysis bag after the dissolution experiments showing agglomeration of the NPs and no change in the size of the primary particles.

Figure 2c. The stability of the suspension decreased with increasing pH (Figure 2c). The point of zero charge for ^{65}CuO-s NPs was found to be around pH 9.5 and for ^{65}CuO-r NPs at pH 8.

Copper Release Study. Nanoparticles with different dissolution characteristics can also be prepared using this protocol. Dissolution was measured in 1 mM $NaNO_3$ (pH = 6.7) solution using dialysis membranes with a low molecular weight cut off value (MWCO =12.4 kDa) in order to effectively only allow the passage of free/complexed dissolved/ionic species. Aliquots for dissolved copper measurements were collected from outside the dialysis bag, which minimized any risk of spillage of CuO NPs suspension from inside the bag to the outside solution and allowed data to be gathered for the entire duration of the study from the same individual sample. Soluble copper nitrate compound were used as controls in the experiment. Equilibrium concentrations of dissolved copper were found to be significantly different between ^{65}CuO-s and ^{65}CuO-r NPs (Figure 3). Dissolved copper of up to 1.3 ppm and 0.4 ppm was released from ^{65}CuO-s and ^{65}CuO-r NPs within 72 h., respectively, which represent 3.5% and 1% in terms of mass % dissolution (Figure 3b). For ^{65}CuO-s NPs an apparent equilibrium Cu concentration was reached within 24 h, from the start of the experiment and no significant change was observed for the remaining duration of the experiment. However, in the case of ^{65}CuO-r apparent equilibrium Cu concentration was only reached after 60 h. Following the dissolution experiment, TEM images of NPs suspensions from inside the dialysis bag (Figure 3c) confirmed the presence of particles with no apparent change in their size. Diffusion of Cu^{2+} through the dialysis bag from the soluble Cu compound was much faster and higher compared with the synthesized NPs, with up to 95% Cu recovery within 10 h (Figure 3b). The dissolution data obtained for the samples were described by a modified first-order reaction rate equation of the form:

$$y(t) = y_{\text{final}}(1 - \exp^{-kt}) \quad (1)$$

With $y(t)$ the released amount of copper (ppm), y_{final} the final steady state concentration of the released copper, k the rate

dx.doi.org/10.1021/es2039757 | Environ. Sci. Technol. 2012, 46, 1216–1222

coefficient, and t the time in hours. The values for y_{final} and k were extracted from the data (selected through least-squares fitting). The rate coefficient of dissolution curve for the samples followed the order of $k_{Cu^{2+}}$ (1.64 h^{-1})> $k^{65}{}_{CuO\text{-}s}$ (0.49 h^{-1})> $k^{65}{}_{CuO\text{-}r}$ (0.050 h^{-1}), which further highlights difference in the dissolution behavior between spherical and rod shaped NPs. The release of Cu^{2+} was fastest from the ionic source, followed by the ^{65}CuO-s NPs and slowest for the ^{65}CuO-r NPs. Such observations are important in testing bioaccumulation and toxicity of nanoparticulate system as different dissolution rates of copper need to be taken into account while interpreting the results or more importantly while designing experiments. The increased dissolution of the copper oxide NPs compared to the bulk copper oxide particles (Supporting Information), is in line with results for titanium dioxide,[15] galena,[16] and zinc oxide[17,18] NPs. Such results are typically attributed to differences in surface area of the particles.[14] However, increased surface area alone cannot explain the differences in the dissolution between the spherical (60 m^2/g) and rod shaped NPs (51 m^2/g). The relative difference in the zeta potential of the rod and spherical NPs points to a lower colloidal stability of rods and thus higher potential for agglomeration of the rods. If agglomeration reduces specific surface area, then it could potentially retard the dissolution[19] and the diffusion of metal ions.[17,20]

Biouptake Studies for ^{65}CuO-s NPs. To determine whether isotopically enriched ^{65}CuO NPs enhances detection of Cu uptake in animal tissues after short waterborne exposures, freshwater snails (*Lymnaea stagnalis*) were exposed for a period of 24 h to different concentrations of ^{65}CuO-s NPs in moderately hard synthetic water (US EPA 2002). Copper concentrations in soft tissues were then inferred from each Cu isotope using ICP-MS. The net uptake of ^{65}Cu in *L. stagnalis* (open circles, Figure 4) was linear over a wide range of concentrations that encompasses most environmental exposures; <150 ppb. In the absence of an isotopic label, Cu accumulation was not detectable until a much higher exposure concentration (solid circles, Figure 4). The effect of the high background Cu concentration (34 $\mu g/g$ in *L. stagnalis*) was circumvented by using isotopically modified NPs, which enhances the detection sensitivity down to environmentally relevant concentrations. A recent study by Dybowska et al.[21] similarly demonstrated by using isotopically modified ^{67}ZnO NPs that uptake of Zn can be measured even at low exposure concentrations despite high Zn background concentrations.

In summary, the results demonstrated in this work clearly shows the advantage of using isotopically enriched nanoparticles over nonenriched nanoparticles for various ecotoxicological studies, wherein low exposure concentrations are required. Cu accumulation was detected with much greater sensitivity if the confounding influence of the Cu background was removed by working with labeled particles. The use of isotopically modified NPs not only provides the ability to detect but also to quantify the bioaccumulation of these NPs inside an organism at environmentally realistic concentrations. The results from this study also demonstrate a robust synthesis method allowing the preparation of spherical and rod shaped ^{65}CuO NPs. The colloidal stability of the particles in different media and the release of soluble copper from the NPs was significantly different, depending on the shape of the ^{65}CuO NPs.

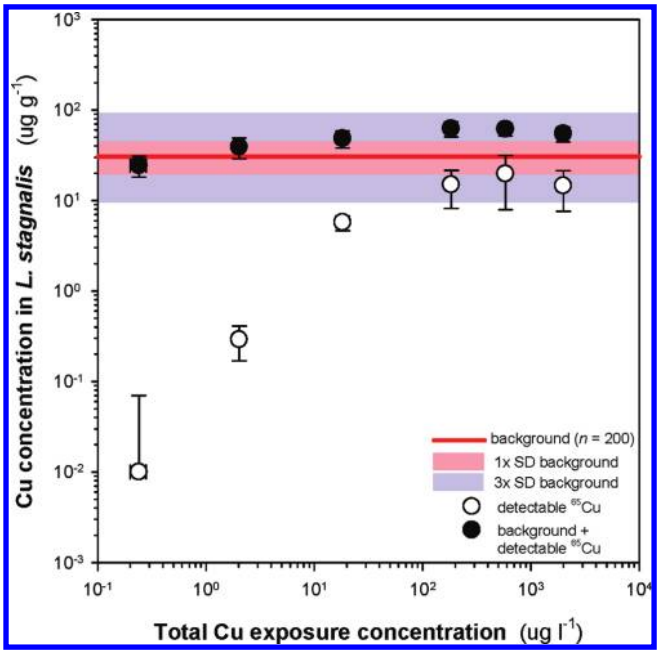

Figure 4. Copper concentrations in snails exposed for 24 h to ^{65}CuO NPs dispersed in synthetic freshwater–water. The red line across the exposure concentrations displays the mean background Cu concentration (total Cu) measured in 200 snails. The shaded areas represent the error surrounding the averaged Cu concentration; 1× (pink) and 3× (blue) the SD of the mean. The open symbols represent the detectable ^{65}Cu (newly accumulated) after exposure to spherical isotopically modified ^{65}CuO NPs. Each concentration was derived from the total measured ^{65}Cu concentrations minus background. The closed symbols represent the sum of the detectable ^{65}Cu, and the background Cu concentrations.

■ ASSOCIATED CONTENT

Ⓢ Supporting Information

The increased dissolution of the copper oxide NPs compared to the bulk copper oxide particles. This material is available free of charge via the Internet at http://pubs.acs.org.

■ AUTHOR INFORMATION

Corresponding Author

*Fax: +44 (0)20 79425537; e-mail: s.misra@nhm.ac.uk.

■ ACKNOWLEDGMENTS

The authors acknowledge Leverhulme Trust (F/00 696/N) for the funding of this project.

■ REFERENCES

(1) Luoma, S. N.; Rainbow, P. S. Why is metal bioaccumulation so variable? Biodynamics as a unifying concept. *Environ. Sci. Technol.* **2005**, *39*, 1921.

(2) Nanotechnology White Paper EPA 100/B-07/001; United States Environmental Protection Agency: Washington DC, 2007; http://www.epa.gov/osa/pdfs/nanotech/epa-nanotechnology-whitepaper-0207.pdf

(3) Wiesner, M. R.; Lowry, G. V.; Casman, E.; Bertsch, P. M.; Matson, C. W.; Di Giulio, R. T.; Liu, J.; Hochella, M. F. Jr. Meditations on the ubiquity and mutability of nano-sized materials in the environment. *ACS Nano* **2011**, *5*, 8466.

(4) Croteau, M. N.; Luoma, S. N.; Topping, B. R.; Lopez, C. B. Stable metal isotopes reveal copper accumulation and loss dynamics in the freshwater bivalve *Corbicula*. *Environ. Sci. Technol.* **2004**, *38*, 5002.

(5) Gulson, B.; Wong, H. Stable isotopic tracing—A way forward for nanotechnology. *Environ. Health Persp.* **2006**, *114*, 1486.

(6) Handler, R. M.; Beard, B. L.; Johnson, C. M.; Scherer, M. M. Atom exchange between aqueous Fe(II) and goethite: An Fe isotope tracer study. *Environ. Sci. Technol.* **2009**, *43*, 1102.
(7) Baek, Y. B.; An, Y. J. Microbial toxicity of metal oxide nanoparticles (CuO, NiO, ZnO, and Sb_2O_3) to *Escherichia coli*, *Bacillus subtilis*, and *Streptococcus aureus*. *Sci. Total Environ.* **2011**, *409*, 1603.
(8) Borkow, G.; Gabbay, J. Putting copper into action: Copper-impregnated products with potent biocidal activities. *FASEB J.* **2004**, *18*, 1728.
(9) Kasemets, K.; Ivask, A.; Dubourguier, H. C.; Kahru, A. Toxicity of nanoparticles of ZnO, CuO, and TiO_2 to yeast Saccharomyces cerevisiae. *Toxicol. In Vitro* **2009**, *23*, 1116.
(10) Aruoja, V.; Dubourguier, H. C.; Kasemets, K.; Kahru, A. Toxicity of nanoparticles of CuO, ZnO, and TiO_2 to microalgae *Pseudokirchneriella subcapitata*. *Sci. Total Environ.* **2009**, *407*, 1461.
(11) Ahamed, M; Siddiqui, M. A; Akhtar, M. J.; Ahmad, I.; Pant, A. B.; Alhadlaq, H. A. Genotoxic potential of copper oxide nanoparticles in human lung epithelial cells. *Biochem. Biophys. Res. Commun.* **2010**, *396*, 578.
(12) Karlsson, H. L.; Gustafsson, J.; Cronholm, P.; Moller, L. Size-dependent toxicity of metal oxide particles-A comparison between nano- and micrometer size. *Toxicol. Lett.* **2009**, *188*, 112.
(13) Studer, A. M.; Limbach, L. K.; Van Duc, L.; Krumeich., F.; Athanassiou, E. K.; Gerber, L. C.; Moch, H.; Stark, W. J. Nanoparticle cytotoxicity depends on intracellular solubility: Comparison of stabilized copper metal and degradable copper oxide nanoparticles. *Toxicol. Lett.* **2010**, *197*, 169.
(14) Gunawan, C.; Teoh, W. Y.; Marquis, C. P.; Amal, R. Cytotoxic origin of copper(II) oxide nanoparticles: Comparative studies with micron-sized particles, leachate, and metal salts. *ACS Nano* **2011**, *5*, 7214.
(15) Schmidt, J.; Vogelsberger, W. Dissolution kinetics of titanium dioxide nanoparticles: The observation of an unusual kinetic size effect. *J. Phys. Chem. B* **2006**, *110*, 3955.
(16) Liu, J.; Aruguete, D. M.; Jinschek, J. R.; Rimstidt, J. D.; Hochella, M. F. The non-oxidative dissolution of galena nanocrystals: Insights into mineral dissolution rates as a function of grain size, shape, and aggregation state. *Geochim. Cosmochim. Acta* **2008**, *72*, 5984.
(17) Bian, S. W.; Mudunkotuwa, I. A.; Rupasinghe, T.; Grassian, V. H. aggregation and dissolution of 4 nm ZnO nanoparticles in aqueous environments: Influence of pH, ionic strength, size, and adsorption of humic acid. *Langmuir* **2011**, *27*, 6059.
(18) Meulenkamp, E. A. Size dependence of the dissolution of ZnO nanoparticles. *J. Phys. Chem. B* **1998**, *102*, 7764.
(19) Peng, X.; Palma, S.; Fisher, N. S.; Wong, S. S. Effect of morphology of ZnO nanostructures on their toxicity to marine algae. *Aquat. Toxicol.* **2011**, *102*, 186.
(20) Liu, J.; Sonshine, D. A.; Shervani, S.; Hurt, R. H. Controlled release of biologically active silver from nanosilver surfaces. *ACS Nano* **2010**, *4*, 6903.
(21) Dybowska, A. D.; Croteau, M. N.; Misra, S. K.; Berhanu, D.; Luoma, S. N.; Christian, P.; O'Brien, P.; Valsami-Jones, E. Synthesis of isotopically modified ZnO nanoparticles and their potential as nanotoxicity tracers. *Environ. Pollut.* **2011**, *159*, 266.